



Tuning Criteria of Nonlinear Flexible Rotor Mounted on Squeeze Film Damper Using Analytical Approach

Karimulla Shaik¹ · B. K. Dutta¹

Received: 26 March 2020 / Revised: 5 June 2020 / Accepted: 17 July 2020 / Published online: 6 August 2020
 © Krishtel eMaging Solutions Private Limited 2020

Abstract

Purpose A close form solution was developed in this paper to find the nonlinear tuning parameters of symmetric/asymmetric rotor—Squeeze film damper system.

Methods Initially, close form solution was developed to find the optimum tuning criteria using linear models. Later, it has been extended to nonlinear unbalanced rotor damper system using circular centre orbit condition. Analytical modeling of Squeeze film damper forces is carried out considering viscous, inertial and temporal contributions under laminar and turbulent conditions. Modified Reynolds equation with short damper approximation is used to derive the SFD forces for 2π -film. The solution of the system of equations helped to predict optimum tuning parameters, such as cross-over frequency and maximum possible amplitudes. Contributions of various governing parameters are discussed.

Conclusion Mass ratio of damper-to-rotor mass and nonlinear radial/tangential damper forces play an important role in finding the tuning parameters of symmetric system. Additional shaft parameter, f_p , plays an important role in getting the optimum tuning parameters of asymmetric system as compared to symmetric system.

Keywords Flexible rotor · Squeeze film dampers · Nonlinear fluid forces · Tuned mass damper

List of symbols

M_s	Mass of rotor and disc system, Kg, $M_s = M$ for asymmetric system, $M_s = M/2$ for symmetric system
M_s	$M/2$ for symmetric system
M	Mass of disc, kg
M_d	Mass of damper, kg
$K1$	Shaft stiffness of top half-length of shaft, N/m
$K2$	Shaft stiffness of bottom half-length of shaft, N/m
$K3$	Stiffness of retainer spring, N/m
K_s	Stiffness of the shaft, N/m $K_s = K1 + K2$ for asymmetric system $K_s = (K1 + K2)/2$
u	Unbalance eccentricity, m
U	Unbalance parameter, $\frac{u}{c}$
ω_n	Natural frequency of rotor, $\sqrt{\frac{K_s}{M_s}}$, Hz

ω_d	Natural frequency of damper, $\sqrt{\frac{K_3}{M_d}}$, Hz
ω_p	Natural frequency of bottom half of the shaft, $\sqrt{\frac{K_2}{M_s}}$, Hz
n	Stiffness ratios of top and bottom half of the shaft, $\frac{K_2}{K_1}$
f	Frequency ratio of damper vs rotor, $\frac{\omega_s}{\omega_n}$
f_p	Frequency ratio of half of the shaft connected at damper end, $\frac{\omega_p}{\omega_n}$
α	Mass ratio of damper to rotor, $\frac{M_d}{M_s}$
ω	Rotational speed, rad/s
Ω	Frequency ratio, ω/ω_n
Cd	Damping coefficient of damper, $2\xi M_d \omega_d$, N-s/m
CC	Critical damping, $2M_d \omega_d$
ξ	Damping ratio, Cd/CC
x_s, y_s, x_d, y_d	Rotor and damper Displacements in Cartesian coordinates, m
$\bar{x}_s, \bar{y}_s, \bar{x}_d, \bar{y}_d$	Non-dimensional rotor and damper displacement in Cartesian coordinates, $\bar{x}_s = \frac{x_s}{c}$, $\bar{y}_s = \frac{y_s}{c}$, $\bar{x}_d = \frac{x_d}{c}$, $\bar{y}_d = \frac{y_d}{c}$
$\mathbf{x}_s, \mathbf{x}_d$	Rotor and damper displacement vector, i.e., $\bar{\mathbf{x}}_s = \bar{x}_s + i\bar{y}_s = \varepsilon_s e^{i\varphi_s}$ and $\mathbf{x}_d = x_d + iy_d = e_d e^{i\varphi_d}$

✉ Karimulla Shaik
 skarim@barc.gov.in
 B. K. Dutta
 bk Dutta@barc.gov.in

¹ Homi Bhabha National Institute (HBNI), Mumbai 400 094, India

\bar{X}_s, \bar{X}_d	Non-dimensional rotor and damper displacement vector
P	Gauge pressure in the damper, N/m ²
m	Dynamic viscosity of damper oil, N-s/m ²
ρ	Density of damper oil, kg/m ³
h	Thickness of the film, m
θ	Angular coordinate measured from the position of maximum film thickness in the direction of rotor angular speed, rad
t	Time, s
R	Radius of damper, m
L	Length of the damper, m
z	Axial coordinate in length direction
φ_s	Angle of rotor from positive- x axis of the Cartesian coordinate system
φ_d	Angle of damper from positive - x axis of the Cartesian coordinate system
c	Initial radial clearance in the damper, m
btt	Tangential damping coefficient, N-s/m
mr cen	Mixed temporal and convective origin in radial direction
$\varepsilon_d \dot{\varphi}_d$	Tangential velocity, rad/s
$\varepsilon_d \dot{\varphi}_d^2$	Centripetal acceleration, rad/s ²
$(\varepsilon_d \dot{\varphi}_d)^2$	Nonlinear tangential acceleration, rad/s ²
F_r, F_t	Damper oil film forces in radial and tangential direction, N
F_{dx}, F_{dy}	Damper oil film forces in x - and y -direction, N
\bar{F}_r, \bar{F}_t	Non-dimensional radial and tangential forces
$\bar{\mathbf{F}}_d$	Non-dimensional force vector, $\bar{F}_{dx} + j\bar{F}_{dy}$
B	Damper viscous parameters, $\frac{4\mu RL^2}{M_s c^3 \omega_n}$
B_I	Damper inertial parameters, $\frac{4\rho RL^3}{M_s c}$
(.)	Denotes differentiation with respect to ' t '
O_g	Mass center of disc
O_s	Geometric center of disc
O_d	Geometric center of damper
O_b	Bearing center
$X-, Y-$	Stationary Cartesian coordinate system with origin at the damper geometric center
$r-, t-$	Rotating coordinate system with origin at the damper geometric center

Subscripts

S	Rotor
d	Damper
r	Radial
t	Tangential
P, Q	Cross-over points in frequency domain

Introduction

A high-speed rotating machinery in general requires additional external damping in addition to ball bearings. Such arrangement helps to reduce the synchronous response of the rotor; when damping provided by the bearings is insufficient to cross through the critical speeds. Tuned mass damper (TMD) systems are also known as dynamic vibration absorber (DVA) are widely used to reduce the vibration of primary system by adding an auxiliary mass on to it. This consists of an auxiliary spring—mass system attached to main system. It results in two-degrees of freedom system. The determination of optimum parameters like stiffness, mass and optimum damping of auxiliary system which leads to lowest possible rotor amplitudes and corresponding transmitted forces over a range of speed is important in the design of rotor–bearing damper systems.

Den Hartog [1] introduced tuning criteria to reduce the amplitude of a single degree freedom (SDOF) system subjected to sinusoidal excitation by incorporating TMD. It was found that frequency of the auxiliary system should be the same as that of main system to get the equal cross-over points leading to lowest amplitude response of the main system. Criteria to get optimum damping were obtained using perturbation method. Randall et al. [2] used numerical search approach to find the optimum cross-over points of the linear TMD system with various parameters like mass ratio α , frequency ratio Ω and damping ratio ξ . A surface plot was generated using these parameters to find the optimum point. Study was extended by Liu and Liu [3] by developing close form solution to find the optimum parameters of the two different types of TMD systems known as skyhook damper and ground hook damper systems. A new approach like differentiating a higher order equation was used to get the optimum parameters of linear system. Febbo and Vera [4] analyzed SDOF or 2DOF system with DVA attached to a continuous beam modeled using Euler beam theory. Different optimization techniques were used to find the optimum parameters for more degrees of freedom systems.

Gunter [5] presented analysis of a gas turbine to find response of rotor mounted on flexible support system. It was shown that lower support stiffness with moderate damping is quite effective in minimizing bearing forces at the time of crossing over of bearing critical speeds. Further Kirk and Gunter [6] extended same concept to design a rotor having flexible support which acts like a DVA at the critical speeds. Cunningham et al. [7] showed the design of TMD for rotor mounted on bearings and SFD support. The work includes the determination of damper parameters to get equal cross-over points of bending critical speeds. Short Bearing Approximation (SBA) is used to find the damper stiffness and damping at fixed eccentricity ratio. Pilkey et al.



[8] developed an efficient two stage method to find the optimum parameters of rotor mounted on a TMD. Damper support forces are used to calculate an equivalent force, which is then used to calculate the TMD parameters. Subsequently, the same can be converted back to equivalent spring mass system to account for all the variables in the calculations.

So far rotor and bearings are assumed to be linear and responses of rotor and bearing are independently predicted. To calculate the damper response, it is desirable to consider nonlinear damper fluid forces at the same instant. Open literature is available [9, 10] to solve the system of nonlinear equations of rotor–damper system using higher order time marching numerical schemes. These time domain solutions can be used to find the asynchronous vibration of the system more accurately. Literature discussed here considers vibration model of rotor–damper system, where rotor mass, damping and stiffness is an equivalent model parameters of actual system. To account for complexity of rotor models, rotor can be modeled using beam theory with finite element method (FEM), where as bearing, dampers and support flexibility can be modeled as spring–damper system and attached at the bearing locations as discussed in more detail [11]. However, additional efforts are required to conduct parametric studies of different variables to find their optimum values to cross over bending critical speeds. Rabinowitz and Hahn [12] developed close form coupled solution of rotor mounted on nonlinear SFD under circular center orbit (CCO) conditions in polar coordinates. Responses of a two-degree flexible rotor and damper system were plotted in terms of various parameters, like α , Ω , U and damping parameters, to get the stable operation. This work has been extended further by Rabinowitz and Hahn [13] to find the TMD parameters of the rotor. Only 2π film approximation can lead to equal cross-over points of TMD. A design chart has been developed to find the optimum parameters at various operating speed. An experimental setup developed by Rabinowitz and Hahn [14] to validate the above results found results in good agreement. Nonlinear programming techniques were used to optimize the SFD mounted on rotor–bearing system to get low cross-over points of critical bending and maximization of instability onset speeds. McLean and Hahn [15] extended this method to solve multi-degree of freedom system simultaneously to find the damper and rotor responses. Results are demonstrated with 2dof system to find the bi-stable operations of SFD. Mclean and Hahn [16] considered fluid stiffness and damping implicitly to investigate the rotor–damper system stability under CCO conditions. The above concepts are extended further to solve the rotor damper responses using finite element method by Chen et al. [17]. Zhu et al. [18] used similar approach to find the multiple solutions of rotor mounted on two similar nonlinear squeeze film dampers operating under CCO conditions. Synchronous and non-synchronous regions of vibrations were predicted. EI-Shafei

and Yakoub [19] studied optimization of multimode rotor mounted on SFD to minimize the amplitude response of the rotor at critical speed and also to minimize the force transmitted to the structures at the operating speed under CCO conditions.

Pietra and Adiletta [20, 21] conducted the review of SFD in two parts. First part reviews the characteristics of SFD, which includes, finding of fluid forces with and without inertia effects, short bearing and long bearing approximation with different boundary conditions of seals, oil inlet and outlet flow, CCO and orbits with small and larger amplitudes and experimental investigations. Second part of review includes the analysis of rigid and flexible rotors mounted on SFD, which includes, responses of rigid-damper system, flexible rotor–damper system in polar and Cartesian coordinate system, nonlinear tuning of rotor–damper symmetric system, stability of rotor–damper system, multi-degree of freedom system and scope for improved designs of SFD includes the floating ring, spiral foil and integral SFD with tilting pads, etc. To improve the performance of SFD, various new design concepts have been proposed in literature. Central circumferential grooves are commonly used to create the positive pressure on damper by external pressure. It divides the film land into two axial lengths, operates independently with constant pressure in the groove. Along with axial flow in the damper, there is circumferential flow in the groove which was considered by Tan et al. [22] to predict forces of squeeze film damper in presence of fluid inertia and results are compared with experiments. Tan and Li [23] extended above work to find the unbalanced response of symmetric flexible rotor mounted on grooved SFD using analytical method. Another popular design includes a thin circular ring placed between outer diameter of the damper and housing known as floating-ring SFD. It can be used to avoid the sub- and super-harmonic rotor damper system. As a part, Rezvani and Hahn [24] conducted experiments to find response of flexible horizontal rotor mounted on asymmetric supports. Model includes uniform shaft with centrally mounted disc with ball bearings at one end of the shaft and ball bearing with SFD without central spring on the other end of the shaft. Rotor responses measured experimentally are in good agreement with theoretical predictions, however theoretically predicted quasi-static vibration was not observed experimentally. This work was extended to find theoretical response of rotor mounted on floating-ring SFD using transient analysis by Rezvani and Hahn [25]. Response is highly dependent on the stiffness, and on the unbalance, and partly on the mass of the ring, but the damping of the outer ring did not have a significant effect. Zhou [26] presented transient analysis of rotor mounted on ball bearings with floating-ring SFD and results are compared with the experiments. It shows that the floating ring inside the SFD will have added advantages over plain SFD, which includes

the preventing of bi-stable operation. Non-synchronous stability can be controlled with floating ring mass. Further concepts of two-lobe bearing have been extended to SFD to find the improved stability of rotor–damper system. Adiletta [27] analyzed theoretically the advantages of two-lobe wave squeeze film damper.

Traditional SFD lubrication oil can be replaced with magneto rheological (MR) fluid to build a variable damping SFD by magnetic/electric field to control the rotor vibration more effectively. Wang et al. [28] presented solution of Reynolds equation of the MR fluid squeeze film using Bingham model to find oil force, and the magnetic pull force. Response of rigid rotor mounted on MR fluid damper is analyzed theoretically to show improved vibration control. Zapomel et al. [29] presented bilinear theoretical material model to represent the MR fluid for better approximation.

Active magnetic bearing (AMB) reached sufficient maturity to replace the conventional hydrodynamic bearings to avoid the high-speed instabilities of rotor bearing system and other advantages like balancing, resonance jumping, etc. Srinivas et al. [30] presented review of AMB, which summarized the basic feature of AMB, various flexible rotor test rigs available in literature and its instrumentation, future research directions. Heidari and Safarpour [31] presented theoretical model for an active squeeze film damper (ASFD) which is a combination of AMB and SFD to control the rotor vibration using variable force, change in fluid film stiffness and damping. Rigid rotor mounted on ASFD is presented to control the jump phenomena and reduced transmitted forces.

Most of the practical systems are horizontal in nature; different types of centering rings are used to keep the rotor system in geometric center. Literature discussed above considers retainer spring as a stiffness element, linear stiffness properties of the spring considers for the calculations. Han et al. [32] presented response of rigid Jeffcott rotor mounted on elastic centering ring SFD, where fluid film of damper was modeled using Reynolds equation and elastic centering ring is modeled using FEM with Kirchhoff assumption. Coupled solution shows that present model prevents bi-stable vibration of rotor by suppressing nonlinear effects of SFD fluid film. However, squirrel cage-type centering spring is commonly used in high-speed aero-engines. Zhang et al. [33] presented multi-objective optimal design method to optimize the squirrel cage-type centering spring, when flexible rotor mounted on SFD with centering spring. Spring mass system is used to model the rotor and damper system, where as nonlinear fluid force of SFD was modeled using analytical solution of reduced Reynolds equation. Length, width, thickness and no. of squirrel cage bars were considered as variables to optimize the stress and stiffness of the centering spring. Results are compared with experiments and are in good agreement.

Literature discussed above summarizes modeling of flexible rotors mounted on various types of passive SFD to reduce the synchronous vibration of rotor. It also includes the advanced SFD with MR fluid and its active control systems. Due to highly nonlinear behavior of SFD, designer needs to optimize the rotor–damper system to get the optimum rotor and damper parameters. The close form solutions can help the designers to get the quick optimum solution, to generate the initial conditions to nonlinear transient solutions and also help to find limits or bounds in optimization studies of the these nonlinear systems. Open literatures documented shows, how to find the optimum parameters of nonlinear symmetric horizontal rotor–damper system to cross over bending critical speed smoothly. These design philosophies were adopted in gas turbines, heavy duty compressors, to operating successfully beyond its bending critical speeds. However, it has been found that not much of literature available in the open domain to find the optimum tuning parameters of asymmetric rotor bearing and damper system. The objective of the present work is to develop a close form solution of nonlinear flexible rotor–damper system to find optimum tuning parameters directly without using optimization techniques. Difference in design philosophy of symmetric and unsymmetrical rotor has been also dealt with examples.

Linear Modeling of Flexible Rotor–Damper System to Find Tuning Conditions

Mathematical modeling of vertical flexible rotor mounted on SFD has been described in this section. Figure 1a shows the schematic diagram of a rotor mounted with a SFD. A mass-less shaft with one central disc was supported at either ends on ball bearings. One end of the ball bearing is mounted with squeeze film damper (SFD) with a retainer spring and another end is directly mounted on housing with ball bearing. Equivalent spring mass system is shown in Fig. 1b. The motion of the system is described by x and y displacements of the geometric center of the damper and rotor disc. External forces acting on the disc are the unbalance and damping forces at the bottom damper. o_d is the center of geometry of the damper, o_s is the center of geometry of the disc and o_g is the center of gravity of the disc. Equation of motion of rotor–damper system is derived with the following assumptions.

- Mass-less shaft mounted with a disc at the mid-span of the rotor shaft having a lumped mass,
- Gravitational effects are neglected,
- Rotor and support stiffness are radially symmetric and linear,
- Rotor imbalance is defined in a single plane on the disc at the rotor mid-span,
- Gyroscopic effect is neglected,

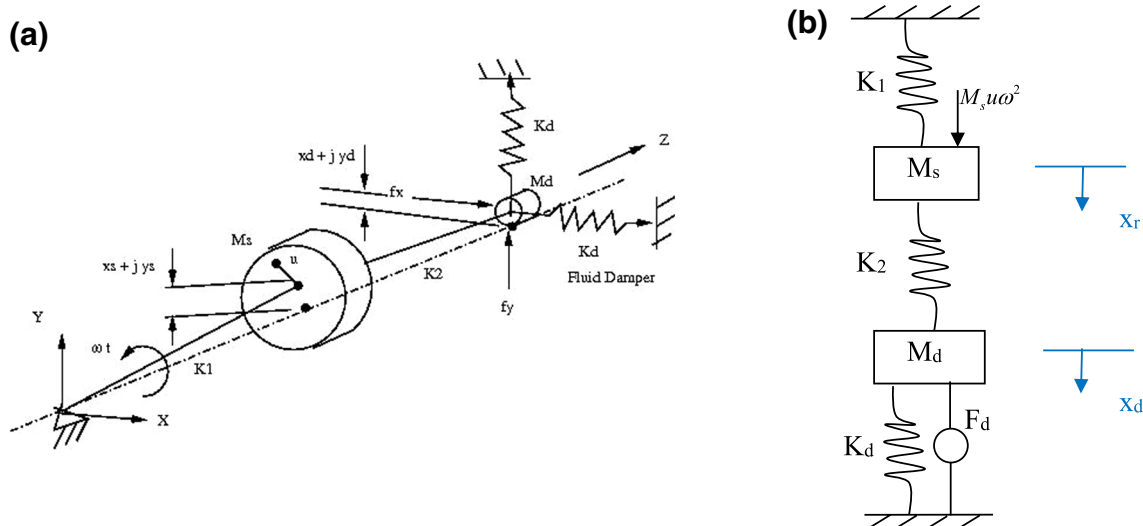


Fig. 1 a Flexible asymmetric rotor mounted on rigid bearings at one end and rigid bearings bearing followed by squeeze film damper, retainer spring on other end. b Equivalent spring, mass and force system

- Roller element bearings are assumed to be rigid,
- Axial and tensional vibrations of the rotor system and the influence of the rolling element bearings are neglected,
- Inertia of the fluid is assumed to be small and neglected,
- Damping is assumed to be linear and a function of velocity.

Equations of motions for the rotor and the damper are written as

$$M_s \ddot{x}_s + K_1(x_s) + K_2(x_s - x_d) = M_s u \omega^2 \cos(\omega t),$$

$$M_s \ddot{y}_s + K_1(y_s) + K_2(y_s - y_d) = M_s u \omega^2 \sin(\omega t), \quad (1a)$$

$$M_d \ddot{x}_d - K_2(x_r - x_d) + K_3 x_d + C_d \dot{x}_d = 0,$$

$$M_d \ddot{y}_d - K_2(y_r - y_d) + K_3 y_d + C_d \dot{y}_d = 0. \quad (1b)$$

Asymmetric system described here is similar to rotor-bearing system described in literature [18]. The hydrodynamic bearing is replaced with ball bearings and squeeze film damper.

Substituting $\bar{\mathbf{x}}_s = \bar{x}_s + i\bar{y}_s = \epsilon_s e^{i\varphi_s}$ and $\mathbf{x}_d = x_d + iy_d = e_d e^{i\varphi_d}$ in Eq. (1) and non-dimensionalizing by dividing Eq. (1a) by $M_s c \omega_n^2$, and Eq. (1b) by $M_d c \omega_n^2$, the solution of Eq. (1) is represented as

$$\mathbf{x}_s = \mathbf{X}_s e^{i(\omega t)} \text{ and } \mathbf{x}_d = \mathbf{X}_d e^{i(\omega t)}. \quad (2)$$

Substituting Eq. (2) into Eq. (1), one gets the solutions of the system as given by

$$\frac{\bar{\mathbf{x}}_s}{U} = \frac{(f_p^2 + \alpha f^2 - \alpha \Omega^2) \Omega^2 + (j2\xi \alpha f \Omega) \Omega^2}{(f_p^2 + \alpha f^2 - \alpha \Omega^2)(1 - \Omega^2) - (f_p^2)^2 + (j2\xi \alpha f \Omega)(1 - \Omega^2)}, \quad (3a)$$

$$\frac{\bar{\mathbf{x}}_d}{U} = \frac{f_p^2 \Omega^2}{(f_p^2 + \alpha f^2 - \alpha \Omega^2)(1 - \Omega^2) - (f_p^2)^2 + (j2\xi \alpha f \Omega)(1 - \Omega^2)}. \quad (3b)$$

One can find the undamped response of the system by substituting $\xi = 0$ in Eq. (3). Further, equating undamped rotor system response to zero, i.e., $\frac{\bar{\mathbf{x}}_s}{U} = 0$ leads to the condition,

$$\Omega = \sqrt{\frac{f_p^2}{\alpha} + f^2}. \quad (4)$$

Equation (4) shows the frequency at which undamped rotor amplitude changes its sign. The form of Eq. (3) is $\frac{\bar{\mathbf{x}}}{U} = \frac{A + j\xi B}{C + j\xi D}$. The response, phase and damping of such kind of system can be calculated using the procedure shown in

[1]. Using such procedure, the response of the rotor and damper are then given by

$$\frac{\bar{X}_s}{U} = \sqrt{\frac{(f_p^2 + \alpha f^2 - \alpha \Omega^2)^2 \Omega^4 + \xi^2 (2\alpha f \Omega)^2 \Omega^4}{\left[(f_p^2 + \alpha f^2 - \alpha \Omega^2)(1 - \Omega^2) - (f_p^2)^2 \right]^2 + \xi^2 (2\alpha f \Omega)^2 (1 - \Omega^2)^2}}, \quad (5a)$$

$$\frac{\bar{X}_d}{U} = \sqrt{\frac{(f_p^2 \Omega^2)^2}{\left[(f_p^2 + \alpha f^2 - \alpha \Omega^2)(1 - \Omega^2) - (f_p^2)^2 \right]^2 + \xi^2 (2\alpha f \Omega)^2 (1 - \Omega^2)^2}}. \quad (5b)$$

The invariant points with respect to ξ are given by the condition $\frac{A^2}{c^2} = \frac{B^2}{D^2}$, which leads to

$$(f_p^2 + \alpha f^2 - \alpha \Omega^2)(1 - \Omega^2) = \pm \left[(f_p^2 + \alpha f^2 - \alpha \Omega^2)(1 - \Omega^2) - (f_p^2)^2 \right]. \quad (6)$$

Taking +ve sign in RHS of Eq. (6) leads to a trivial solution $\Omega=0$. On the other hand, considering -ve sign in RHS of the same equation leads to fourth-order polynomial. The roots of the polynomial equation will give cross-over (CO) frequencies at points (P, Q) of the undamped system. This is given by

$$\Omega_{P,Q}^2 = \frac{1}{2} \left(1 + f^2 + \frac{f_p^2}{\alpha} \right) \pm \frac{1}{2} \sqrt{\left(1 + f^2 + \frac{f_p^2}{\alpha} \right)^2 - 4 \left(\frac{f_p^2}{\alpha} - \frac{f_p^4}{2\alpha} + f^2 \right)}. \quad (7)$$

Rigid rotor response of the system can be found out by substituting very large value of ξ , i.e., $\frac{\bar{X}_s}{U} \Rightarrow \infty$. This leads to $\frac{\bar{X}_s}{U} = \frac{B}{D} = \frac{\Omega^2}{1 - \Omega^2}$.

By considering $\left(\frac{\bar{X}_s}{U} \right)_{u=\infty}$, one gets the condition of rigid rotor frequency as

$$\Omega = \pm 1. \quad (8)$$

To get the condition of equal amplitude at CO, one needs to satisfy the following relation, $\frac{\Omega_p^2}{1 - \Omega_p^2} = -\frac{\Omega_Q^2}{1 - \Omega_Q^2}$. This leads to an expression of equal cross-over amplitudes as

$$f^2 = 1 - \frac{f_p^2}{\alpha} (1 - f_p^2). \quad (9)$$

By substituting Eq. (9) into Eq. (7), one gets the frequency at equal cross-over points. Optimum damping is obtained by substituting Eq. (4), Eq. (8) and, Eq. (9) into

Eq. (5a). This leads to an expression of equal amplitude at frequencies at cross-over points as well at rigid critical,

which is shown below:

$$\xi_{\text{opt}}^2 = \frac{f_p^4}{2(\alpha - f_p^2 + f_p^4)}. \quad (10)$$

Equation (10) gives the condition of optimum damping with respective damper mass. Optimum damping required

for respective rotor mass can be described as $\xi_{\text{opt}}^2 = \frac{\alpha f_p^4}{2}$.

The above methodology is extended to symmetric rotor-bearing damper system. For this purpose, a mathematical modeling of flexible rotor mounted on symmetric supports with SFD is described here. A mass-less shaft mounted with a central disc is supported at either ends on identical ball bearings and SFDs with retainer springs as shown in Fig. 2a. An equivalent spring mass system is shown in Fig. 2b. Assumptions described above are also applicable in this case. Equation of motion for the rotor and the damper can be written as

$$M_s c \ddot{\bar{x}}_s + K_s c (\bar{x}_r - \bar{x}_d) = M_s u \omega^2 e^{i\omega t}, \quad (11a)$$

$$M_d c \ddot{\bar{x}}_d - K_s c (\bar{x}_r - \bar{x}_d) + K_3 c \bar{x}_d + C_d c \dot{\bar{x}}_d = 0. \quad (11b)$$

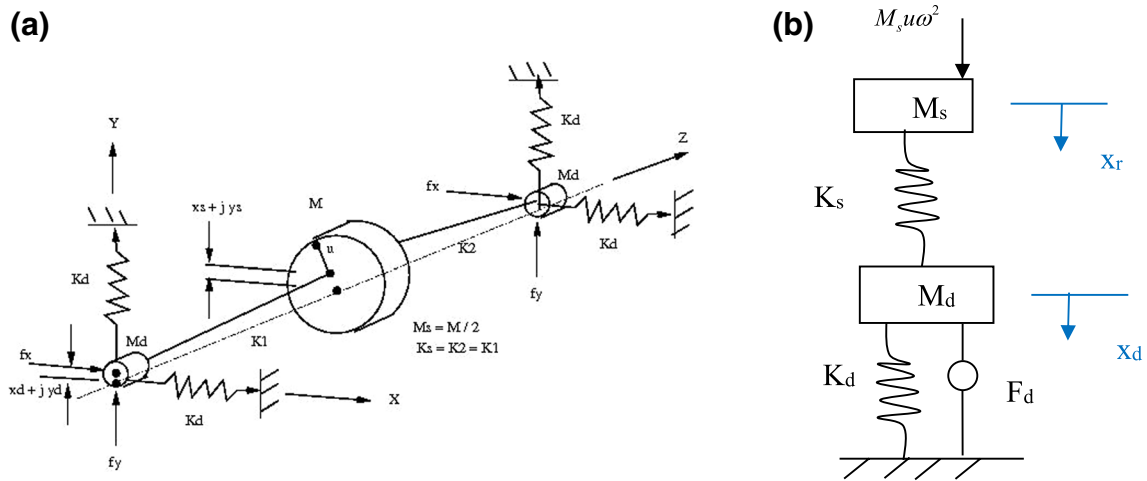


Fig. 2 **a** Flexible symmetric rotor supported on identical squeeze film dampers and retainer springs. **b** Equivalent spring, mass and force system

The solution of Eq. (11) is same as described at Eq. (2). The responses of rotor and damper are given as follows:

$$\frac{\bar{X}_s}{U} = \sqrt{\frac{[1 + \alpha(f^2 - \Omega^2)]^2 (\Omega^2)^2 + \xi^2 (2\alpha\Omega)^2 (\Omega^2)^2}{\langle [1 + \alpha(f^2 - \Omega^2)](1 - \Omega^2) - 1 \rangle^2 + \xi^2 (2\alpha\Omega)^2 (1 - \Omega^2)^2}} \quad (12a)$$

$$\frac{\bar{X}_d}{U} = \sqrt{\frac{(\Omega^2)^2}{\langle [1 + \alpha(f^2 - \Omega^2)](1 - \Omega^2) - 1 \rangle^2 + \xi^2 (2\alpha\Omega)^2 (1 - \Omega^2)^2}} \quad (12b)$$

All other parameters, such as CO frequencies of undamped symmetric system, condition to get the equal CO amplitudes and optimum damping, can be obtained for symmetric system using Eq. (7), Eq. (9) and Eq. (10) by substituting \$f_p = 1\$.

Nonlinear Modeling of Flexible Rotor Damper System to Find Tuning Conditions

Tuning criteria of flexible rotor mounted on SFD described in previous section are further extended to consider the nonlinear fluid forces. All assumptions made in the previous section are also applicable in this case except linear damping and contribution of inertial effect of fluid. The forces generated by oils film of the damper are determined by the Reynolds equation with an incompressible lubricant and short bearing approximation (SBA). The contributions of fluid inertial effects are also considered in this case. The system of all governing equations is solved simultaneously using CCO motion of the system. Free body diagram of rotor–damper model is shown in Fig. 1. EOM about mass center of the rotor and the journal center of damper written in Cartesian coordinates in both the directions are as follows:

$$M_s c \ddot{\bar{x}}_s + K_1 c (\bar{x}_s) + K_2 c (\bar{x}_s - \bar{x}_d) = M_s u \omega^2 e^{i\omega t}, \quad (13a)$$

$$M_d c \ddot{\bar{x}}_d - K_2 c (\bar{x}_s - \bar{x}_d) + K_3 c \bar{x}_d = \bar{F}_d e^{i\omega t}. \quad (13b)$$

The Rotor–damper system is assumed to have the synchronous circular center orbit (CCO) excitation, as shown in Fig. 3. With this assumption, the force and the displacement in \$x\$-direction is orthogonal to \$y\$-direction. The steady-state equilibrium solution of Eq. (13) is given in Eq. (2). Substituting Eq. (2) into Eq. (13), and dividing Eq. (13a) with \$M_s c \omega_n^2\$, and Eq. (13b) with \$M_d c \omega_n^2\$, lead to a set of equations given by

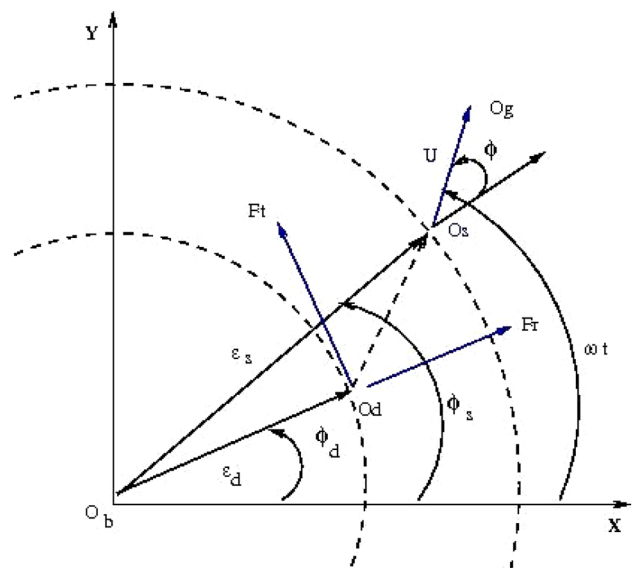


Fig. 3 Circular center orbit motion of rotor–damper system

$$\begin{bmatrix} A_{11} & A_{12} \\ A_{21} & A_{22} \end{bmatrix} \begin{Bmatrix} \bar{\mathbf{X}}_s \\ \bar{\mathbf{X}}_d \end{Bmatrix} = \begin{bmatrix} \bar{\mathbf{F}}_u \\ \bar{\mathbf{F}}_d \end{bmatrix}. \tag{14}$$

Here, subscript ‘*u*’ corresponds to unbalance force and ‘*d*’ corresponds to damper fluid film forces. Other components of the above matrix are $A_{11} = (1 - \Omega^2)$, $A_{12} = A_{21} = -f_p^2$, $A_{22} = (f_p^2 + \alpha f^2 - \alpha \Omega^2)$. The method described in [15] is used here to find the response of the damper. From Eq. (14), one can find the damper force as

$$\bar{\mathbf{F}}_d = \bar{\mathbf{V}} + \bar{\mathbf{E}}\bar{\mathbf{X}}_d, \tag{15}$$

where $\bar{\mathbf{V}} = A_{21}A_{11}^{-1}\bar{\mathbf{F}}_u$ and $\bar{\mathbf{E}} = A_{22} - A_{21}A_{11}^{-1}A_{12}$. The nonlinear damper fluid forces described in next section can be represented in Cartesian coordinates using the following relation:

$$\mathbf{F}_d = F_{dx} + jF_{dy}, \tag{16}$$

where $F_{dx} = \frac{1}{\epsilon_d}(F_r x_d - F_t y_d)$ and $F_{dy} = \frac{1}{\epsilon_d}(F_r y_d + F_t x_d)$. The relation between damper force F_d and displacement X_d can be written as:

$$\bar{\mathbf{F}}_d = \frac{1}{\epsilon_d}(\bar{F}_r + j\bar{F}_t)\bar{\mathbf{X}}_d = \mathbf{G}\bar{\mathbf{X}}_d. \tag{17}$$

Equating Eq. (16) and Eq. (17) to get the damper response, one gets

$$\bar{\mathbf{X}}_d = \frac{\bar{\mathbf{V}}}{(\bar{\mathbf{G}} - \bar{\mathbf{E}})} = \frac{\bar{V}_{Re} + j\bar{V}_{Im}}{\left(\frac{\bar{F}_r}{\epsilon_d} - \bar{E}_{Re}\right) + j\left(\frac{\bar{F}_t}{\epsilon_d} - \bar{E}_{Im}\right)}. \tag{18}$$

Simplification of Eq. (18) leads to

$$\begin{aligned} &(\bar{F}_r)^2 + (\bar{F}_t)^2 + \epsilon_d^2(\bar{E}_{Re}^2 + \bar{E}_{Im}^2) \\ &- 2\epsilon_d^2[\bar{F}_r\bar{E}_{Re} + \bar{F}_t\bar{E}_{Im}] - (\bar{V}_{Re}^2 + \bar{V}_{Im}^2) = 0. \end{aligned} \tag{19}$$

Bisectional method is used to solve Eq. (19) within the limits of $0 \leq \epsilon_d \leq 1$. Response of the rotor is calculated using Eq. (14) is given by

$$\frac{\bar{\mathbf{X}}_s}{U} = \sqrt{\frac{\left[\left(f_p^2 + \alpha f^2 - \alpha \Omega^2 + \frac{\bar{F}_r}{\epsilon_d}\right)\Omega^2\right]^2 + \left(\frac{\bar{F}_t}{\epsilon_d}\Omega^2\right)^2}{\left[\left(f_p^2 + \alpha f^2 - \alpha \Omega^2 + \frac{\bar{F}_r}{\epsilon_d}\right)(1 - \Omega^2) - \left(f_p^2\right)^2\right]^2 + \left[\frac{\bar{F}_t}{\epsilon_d}(1 - \Omega^2)\right]^2}}, \tag{20}$$

where $\bar{V}_{Re} = -\frac{f_p^2 U \Omega^2}{(1 - \Omega^2)}$ and $\bar{V}_{Im} = 0$.

$$\bar{E}_{Re} = \left(f_p^2 + \alpha f^2 - \alpha \Omega^2\right) - \frac{f_p^4}{(1 - \Omega^2)} \text{ and } \bar{E}_{Im} = 0.$$

Equating undamped rotor response to zero in Eq. (20), i.e., $F_t = 0$, one gets the expression for frequency:

$$\Omega = \sqrt{\frac{f_p^2}{\alpha} + f^2 + \frac{\bar{F}_r}{\epsilon_d}}. \tag{21a}$$

Undamped response of the damper from Eq. (21a) can be obtained as

$$\frac{\bar{X}_d}{U} = -\frac{1}{f_p^2} \left(\frac{f_p^2}{\alpha} + f^2 + \frac{\bar{F}_r}{\epsilon_d} \right). \tag{21b}$$

CO frequencies at *P* and *Q* of an undamped nonlinear asymmetric system is given by

$$\begin{aligned} \Omega_{P,Q}^2 = &\frac{1}{2} \left(1 + f^2 + \frac{f_p^2}{\alpha} + \frac{\bar{F}_r}{\epsilon_d} \right) \pm \frac{1}{2} \\ &\sqrt{\left(1 + f^2 + \frac{f_p^2}{\alpha} + \frac{\bar{F}_r}{\epsilon_d} \right)^2 - 4 \left[\left(1 - \frac{f_p^2}{2} \right) \frac{f_p^2}{\alpha} + f^2 + \frac{\bar{F}_r}{\epsilon_d} \right]}. \end{aligned} \tag{22}$$

Condition to get the equal cross-over amplitudes is

$$f = \sqrt{1 - \frac{f_p^2}{\alpha} \left(1 - f_p^2 \right) - \frac{\bar{F}_r}{\epsilon_d}}. \tag{23}$$

The optimum damping required based on rotor mass is

$$\left(\frac{\bar{F}_t}{\epsilon_d} \right)_{opt}^2 = 2\alpha f_p^4. \tag{24}$$

Tuning criteria of vertical flexible rotor mounted on SFD has been described above. This is extended here to consider symmetric nonlinear system. By using free body diagram of rotor–damper model, as shown in Fig. 2, the EOM can be written as

$$M_s c \ddot{\bar{\mathbf{x}}}_s + K_s c (\bar{\mathbf{x}}_s - \bar{\mathbf{x}}_d) = M_s u \omega^2 e^{i\omega t}, \tag{25a}$$

$$M_d c \ddot{\bar{\mathbf{x}}}_d - K_s c (\bar{\mathbf{x}}_s - \bar{\mathbf{x}}_d) + K_3 c \bar{\mathbf{x}}_d = \mathbf{F}_d e^{i\varphi_d}. \tag{25b}$$

All other parameters, such as damper and rotor response of nonlinear symmetric system, CO frequencies of

undamped nonlinear symmetric system, condition to get the equal CO amplitudes and optimum damping, can be obtained for symmetric system by using Eqs. (19), (20), (22), (23) and (24) after substituting $f_p = 1$. However, a summary of optimum parameters for linear and nonlinear symmetric and asymmetric systems is shown in Table 1.

Dynamic Fluid Force Calculations of SFD

For the present system, the Navier–Stokes (NS) equations can be reduced to Reynolds equations by making following assumptions.

- The oil film thickness is small compared to the radius of the journal, hence, the curvature of the oil film is negligible,
- The pressure gradient along the oil film thickness is small and is neglected,
- The velocity gradient along the oil film thickness is small and is neglected,
- Laminar fluid flow is assumed within the clearance and
- Volumetric fluid force is neglected.

The average axial pressure gradient for short bearing approximation (SBA) including the turbulent effects can be written as [11, 35–37]:

$$\frac{\partial P(\theta, t)}{\partial z} = 12 \left[\tilde{k}_z \frac{\mu}{h^3} \left(\frac{\partial h}{\partial t} \right) + K_{mom} \frac{\rho}{h} \left(\frac{\partial^2 h}{\partial t^2} \right) - K_{eng} \frac{\rho}{h^2} \left(\frac{\partial h}{\partial t} \right)^2 \right] z, \tag{26}$$

where K_{mom} and K_{eng} are constants derived from momentum approximation and energy approximation. In the momentum approximation, K_{eng} is fully convective term and in case of energy equation, K_{eng} has both temporal (1/20) and convective contributions (27/140). In the present work, the corresponding values are taken as $K_{mom} = 1/12$ and $K_{eng} = 1/5$ for momentum approximation and $K_{mom} = 1/10$ and $K_{eng} = 17/70$ for energy approximation. These values are suggested in Ref. [35–37]. The turbulent effect \tilde{k}_z can then be expressed using $\tilde{k}_z = (a_z + b_z \varepsilon \cos \theta)$, where $a_z = 1 + 0.00069Re^{0.888}$ and $b_z = 0.00061Re^{0.888}$. Film thickness ‘ h ’ at any given location of plain damper is given by $h = c(1 + \varepsilon \cos \theta)$. The assumed boundary conditions are one end sealed $\frac{\partial P(0, t)}{\partial z} = 0$ and the other end open $P(L, t) = 0$ due to submerged conditions. Integrating Eq. (26) and substituting boundary conditions, pressure distribution under CCO condition as given by

$$P(\theta, t) = 6 \left[\frac{\mu}{c^2} \left(a_z \frac{\sin \theta}{(1 + \varepsilon \cos \theta)^3} (\varepsilon \dot{\phi}_d) + b_z \varepsilon \frac{\sin \theta \cos \theta}{(1 + \varepsilon \cos \theta)^3} (\varepsilon \dot{\phi}_d) \right) + \rho K_{mom} \left(-\frac{\cos \theta}{(1 + \varepsilon \cos \theta)} (\varepsilon \dot{\phi}_d^2) \right) - \rho K_{eng} \left(\frac{\sin^2 \theta}{(1 + \varepsilon \cos \theta)^2} (\varepsilon^2 \dot{\phi}_d^2) \right) \right] (z^2 - L^2). \tag{27}$$

The components of the forces exerted by the oil fluid, viz. radial F_r and tangential F_t directions are obtained by integrating Eq. (27) along the length and circumferential directions. These expressions are as follows:

$$F_r = -\frac{4\mu RL^3}{c^2} [a_z I_3^{11}(\varepsilon \dot{\phi}_d) + b_z \varepsilon I_3^{12}(\varepsilon \dot{\phi}_d)] + 4\rho RL^3 [K_{mom} I_1^{02}(\varepsilon \dot{\phi}_d^2) + K_{eng} I_2^{11}(\varepsilon^2 \dot{\phi}_d^2)], \tag{28a}$$

and

$$F_t = -\frac{4\mu RL^3}{c^2} [a_z I_3^{20}(\varepsilon \dot{\phi}_d) + b_z \varepsilon I_3^{21}(\varepsilon \dot{\phi}_d)] + 4\rho RL^3 [K_{mom} I_1^{11}(\varepsilon \dot{\phi}_d^2) + K_{eng} I_2^{30}(\varepsilon^2 \dot{\phi}_d^2)]. \tag{28b}$$

Integrals ‘ I ’ in Eq. (28) can be evaluated by using [38]. The expressions for the damping and inertial coefficients for a 2π -film (uncavitated) of SFD are shown in Table 2. Under CCO condition, all acceleration and radial velocity terms in Eq. (28) become zero. Final radial and tangential forces under this condition, non-dimensionalized by dividing with $M_d c \omega_n^2$ and multiplying with α , are shown below:

$$\bar{F}_r = B_1 (K_{mom} + \varepsilon K_{eng}) m_{rcen} \varepsilon \Omega^2, \tag{29a}$$

$$\bar{F}_t = -B b_{tt} \varepsilon \Omega. \tag{29b}$$

Case Studies

The objective of the present work includes finding the non-linear tuning parameters of asymmetric flexible rotor–damper system. A close form solution of linear system was developed to find the optimum parameters to cross the bending critical speeds were discussed. Solution includes the finding conditions to get the required mass ratio, α , cross-over frequencies and equal amplitudes at P , Q and optimum damping required. A close form solution was developed to find the optimum tuning parameters of asymmetric rotor mounted on rigid ball bearings on both the side and followed by SFD at one end. Responses of asymmetric linear rotor mounted on SFD are governed by the following parameters: f, f_p, α, ξ , and Ω . Tuning criteria was made independent from unbalance response by dividing the responses

of the system with unbalance parameters, U . Present model was validated with literature problem [12] for symmetric rotor mounted on SFD. Figure 4 shows response of rotor,

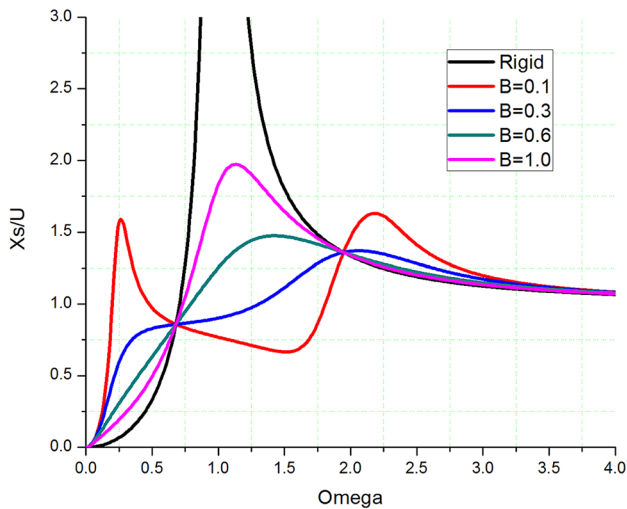


Fig. 4 Responses of nonlinear symmetric rotor [12], ($f=0.1$, $U=0.05$, $\alpha=0.333$ at various values of $B=0.1, 0.3, 0.6, 1.0$)

($\frac{\bar{X}_s}{U}$), at various operating conditions given as, $f=0.1$, $U=0.05$, $\alpha=0.333$ at various values of $B=0.1, 0.3, 0.6, 1.0$. Results are in good agreement with literature problem, Fig. 4b of Ref. [12].

(a) Case Study 1: Analysis of a Linear Asymmetric Rotor–Damper System: Present case study deals with the analysis of a linear asymmetric rotor–damper system. To calculate the results of a linear asymmetric system, the various rotor and damper parameters considered here are stiffness $K_1=K_2=K_3=27,680$ N/m, model stiffness of shaft, $K_s=K_1+K_2$, the disc mass $M_s=1.1072$ kg, $f=0.8165$ and $f_p=0.7071$. The value of $\alpha=0.75$, which is calculated using Eq. (9) for tuning condition of above parameters. The required optimum damping calculated using Eq. (10) is $\xi_{opt}=0.5$ and corresponding $C_d=158$ N s/m. Three different damping ratios are considered here to plot the response of asymmetric rotor and damper. These are under damping case, where $\xi_1=0.5\xi_{opt}$, optimum damping case, ξ_{opt} and over-damping case, where $\xi_2=1.5\xi_{opt}$. Cross-over frequencies are calculated using Eq. (7) as $\Omega P=0.752$ and $\Omega Q=1.330$. The CO amplitudes at P and Q points are obtained for undamped response of the system using Eq. (3a) as 2.65. Figure 5a shows response of rotor, ($\frac{\bar{X}_s}{U}$), for five different conditions. These are the responses of a rigid rotor, undamped tuned rotor, tuned optimum damping, tuned under damping and tuned over damping conditions. The figure also shows the cross-over frequency and amplitudes of the rotor–damper system. Similarly, Fig. 5b shows the response

Table 1 Comparison of tuning criteria of various rotor-support models

Model type	Cross-over frequencies at P, Q	Condition for equal cross-over points	Optimum damping (with main system mass)
Vibration model [1]	$\Omega_{P,Q}^2 = \left(\frac{1+f^2+af^2}{2+\alpha} \right) \pm \sqrt{\left(\frac{1+f^2+af^2}{2+\alpha} \right)^2 - \left(\frac{2f^2}{2+\alpha} \right)}$	$f = \frac{1}{1+\mu}$	$\xi_{opt}^2 = \frac{3\mu}{8(1+\mu)^3}$
Symmetric rotor-damper model (linear)	$\Omega_{P,Q}^2 = \frac{1}{2} \left(1+f^2 + \frac{1}{\alpha} \right) \pm \frac{1}{2} \sqrt{\left(1+f^2 + \frac{1}{\alpha} \right)^2 - 4 \left(f^2 + \frac{1}{2\alpha} \right)}$	$f = 1$	$\xi_{opt}^2 = \frac{1}{2\alpha}$
Symmetric rotor-damper model (nonlinear)	$\Omega_{P,Q}^2 = \frac{1}{2} \left(1+f^2 + \frac{1}{\alpha} + \frac{\bar{F}_r}{\epsilon_d} \right) \pm \frac{1}{2} \sqrt{\left(1+f^2 + \frac{1}{\alpha} + \frac{\bar{F}_r}{\epsilon_d} \right)^2 - 4 \left(f^2 + \frac{1}{2\alpha} + \frac{\bar{F}_r}{\epsilon_d} \right)}$	$f = \sqrt{1 - \frac{\bar{F}_r}{\epsilon_d}}$	$\left(\frac{\bar{F}_r}{\epsilon_d} \right)_{opt}^2 = 2\alpha$
Asymmetric rotor-damper model (linear)	$\Omega_{P,Q}^2 = \frac{1}{2} \left(1+f^2 + \frac{f_p^2}{\alpha} \right) \pm \frac{1}{2} \sqrt{\left(1+f^2 + \frac{f_p^2}{\alpha} \right)^2 - 4 \left(\frac{f_p^2}{\alpha} - \frac{f_p^4}{2\alpha} + f^2 \right)}$	$f = \sqrt{1 - \frac{f_p^2}{\alpha} (1 - f_p^2)}$	$\xi_{opt}^2 = \frac{f_p^4}{2(\alpha - f_p^2 + f_p^4)}$
Asymmetric rotor-damper model (nonlinear)	$\Omega_{P,Q}^2 = \frac{1}{2} \left(1+f^2 + \frac{f_p^2}{\alpha} + \frac{\bar{F}_r}{\epsilon_d} \right) \pm \frac{1}{2} \sqrt{\left(1+f^2 + \frac{f_p^2}{\alpha} + \frac{\bar{F}_r}{\epsilon_d} \right)^2 - 4 \left[\left(1 - \frac{f_p^2}{2} \right) \frac{f_p^2}{\alpha} + f^2 + \frac{\bar{F}_r}{\epsilon_d} \right]}$	$f = \sqrt{1 - \frac{f_p^2}{\alpha} (1 - f_p^2) - \frac{\bar{F}_r}{\epsilon_d}}$	$\left(\frac{\bar{F}_r}{\epsilon_d} \right)_{opt}^2 = 2\alpha f_p^4$

Table 2 Damping and inertial coefficients of 2π -film (uncavitated)

Coef- ficient	Integral coefficients	2π film
b_{tt}	$-(a_z I_3^{20} + b_z \epsilon I_3^{21})$	$-a_z \pi \left[\frac{1}{(1-\epsilon^2)^{\frac{3}{2}}} \right] - b_z \frac{\pi}{\epsilon^2} \left[\frac{(2-3\epsilon^2)}{(1-\epsilon^2)^{\frac{3}{2}}} - 2 \right]$
m_{rcen}	$K_{mom} I_1^{02} + K_{eng} I_2^{21}(\epsilon)$	$K_{mom} \frac{2\pi}{\epsilon^2} \left(\frac{1}{\sqrt{1-\epsilon^2}} - 1 \right) + K_{eng} \frac{2\pi}{\epsilon^2} \left(\frac{\epsilon^2-2}{\sqrt{1-\epsilon^2}} + 2 \right)$

of the damper, $\left(\frac{\bar{x}_d}{U}\right)$, at four different conditions. These are again the responses of undamped tuned damper, tuned optimum damping, tuned under-damping and tuned

over-damping conditions. Over-damping or under damping conditions led to the increase in rotor and damper amplitudes; whereas, optimum damping only can lead to lower amplitude of the rotor–damper system during crossing over of bending critical speeds.

(b) Case Study 2: Analysis of a Linear Symmetric System: Above calculations are modified to find the optimum parameters required for a symmetric system. The various rotor and damper parameters considered here are, the stiffness $K_s = K_1 = K_2 = K_3 = 27,680$ N/m, the disc mass of $M_s = 0.5536$ kg. Both the values f and α are unity for symmetric system. The required optimum damping is calculated as $\xi_{opt} = 0.5$ and the corresponding damping, Cd as 175 N-s/m. As above, three different damping ratios are considered

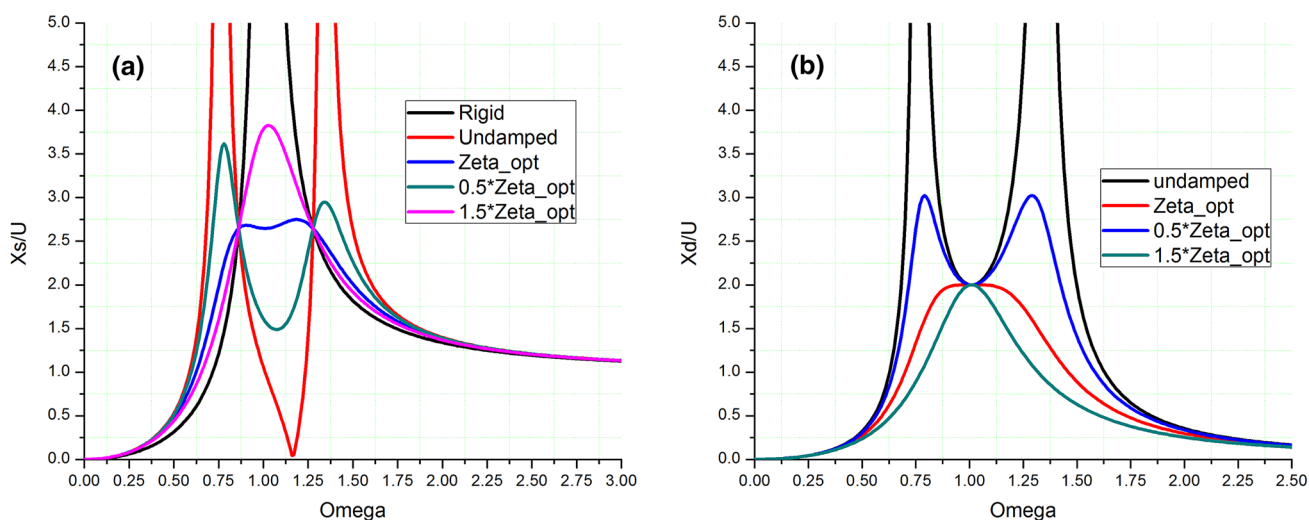


Fig. 5 Results of Case Study-1: **a** responses of linear asymmetric rotor and **b** damper ($f=0.8165, f_p=7071$ and $\alpha=0.75$)

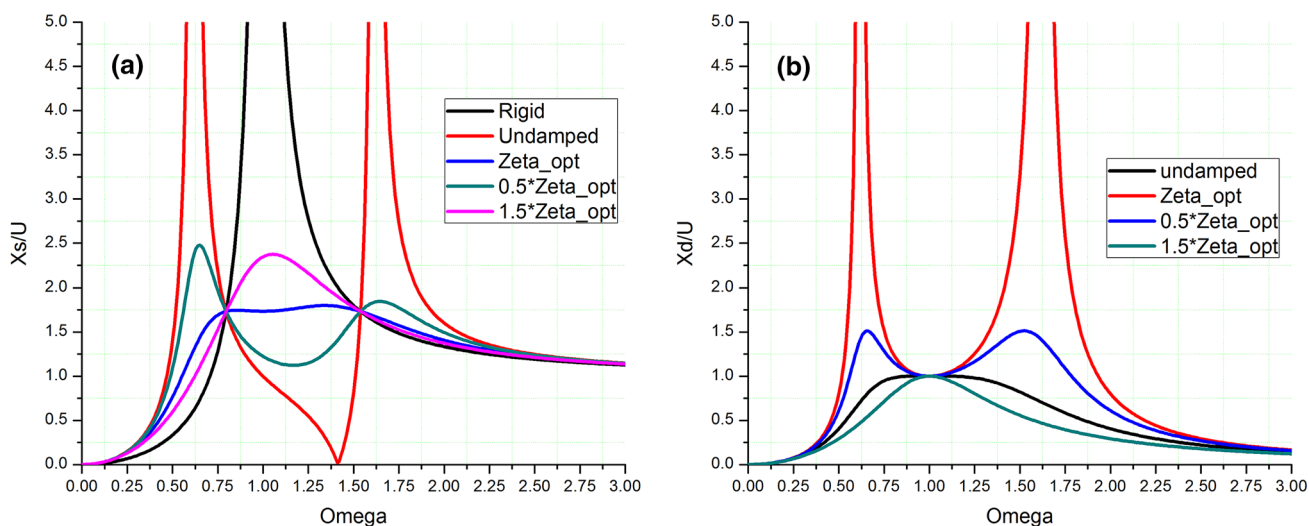


Fig. 6 Results of Case Study-2: **a** responses of linear symmetric rotor and **b** damper ($f=1, \alpha=1$)

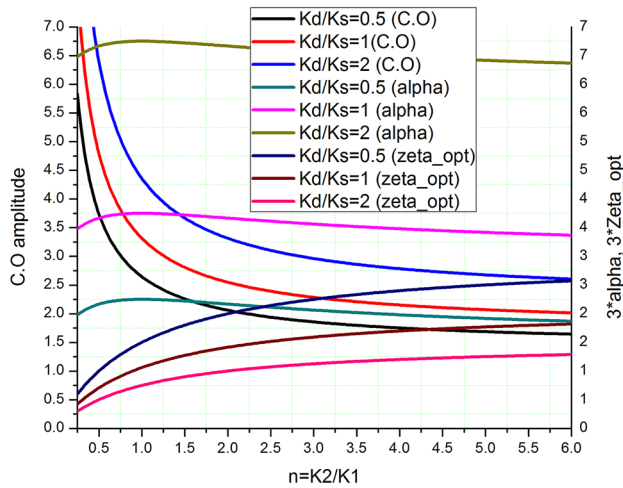


Fig. 7 Result of Case Study-2: ‘*n*’ vs cross-over amplitude, α and ξ_{opt} (linear asymmetric system)

here to plot the rotor–damper response. These are, under-damping case $\xi_1 = 0.5\xi_{opt}$, case of optimum damping ξ_{opt} and over-damping case $\xi_2 = 1.5\xi_{opt}$. Cross-over frequencies are $\Omega P = 0.618$ and $\Omega Q = 1.618$. The corresponding rotor amplitude at cross-over points is 1.732, for undamped system obtained by using Eq. (3a).

Compared to asymmetric system, optimum damping required for symmetric system will be higher. Along the line of Case Study 1, Fig. 6a shows response of symmetric rotor ($\frac{\bar{x}_s}{U}$) at five different conditions. These are, the response of a rigid rotor, the undamped tuned rotor, the tuned optimum damping, the tuned under-damping and the tuned over-damping conditions. It also shows the cross-over frequency and amplitudes of the rotor and damper system. Similarly, Fig. 6b shows the response of the damper ($\frac{\bar{x}_d}{U}$) at four different conditions. These are, undamped tuned damper, tuned optimum damping, tuned under-damping and tuned over-damping conditions. As shown, over-damping or under-damping conditions led to the increase in rotor and damper amplitudes. Only tuned damping leads to lower amplitude of the rotor and damper during crossing over of bending critical speeds.

Parametric study by varying various parameters like ‘*n*’, CO amplitude, α and ξ_{opt} , shows that ‘*n*’ plays an important role in tuning of asymmetric system unlike symmetric system. Figure 7 shows that increase in ‘*n*’ reduce the CO amplitude of rotor. Optimum damper mass increases with increase in the value of ‘*n*’ and then reduces by increasing the value of ‘*n*’. ξ_{opt} increases with the increase in ‘*n*’. The CO amplitude of rotor and tuned damper mass reduce with the decrease in support stiffness, whereas required ξ_{opt} increases with the decrease in support stiffness. The above discussion holds good for symmetric system, which

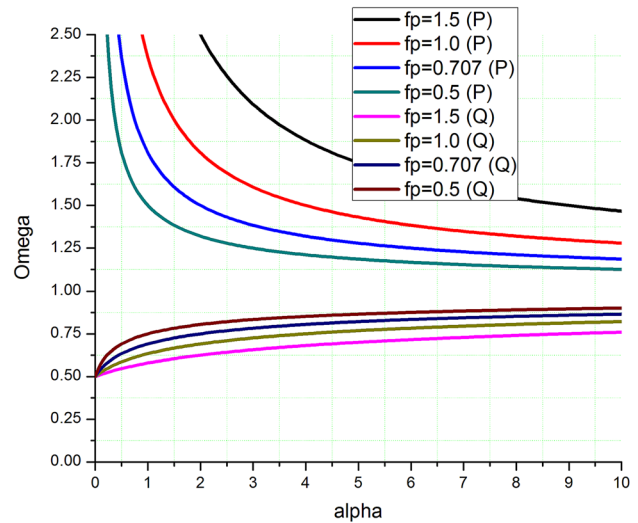


Fig. 8 Result of Case Study-2: α vs cross-over frequencies, $\Omega_{(P,Q)}$

is a special case of asymmetric system where $n = 1$. Figure 8 shows the plot of ‘ α ’ vs splitting frequencies at (P, Q). Difference between split frequencies increase with the increase in f_p . Symmetric system is a special case of asymmetric system with $f_p = 0.7071$ at $\alpha = 0.5$. CO amplitudes of asymmetric system are higher than the symmetric system. Differences between two CO frequencies of asymmetric system are lower than symmetric rotor. However, reduction in retainer spring stiffness causes increase in the difference between CO frequencies and decrease in the CO amplitude of both the symmetric and asymmetric systems.

(c) Case Study 3: Analysis of Nonlinear Asymmetric Rotor and Damper System: Uncavitated film with 2π film approximation is used to find tangential and radial forces with viscous, inertial, temporal contributions under laminar and turbulent conditions. Both momentum and energy approximations are used to resolve the temporal and convective contributions in the theoretical model. It leads to constants $K_{mom} = 1/12$ and $K_{eng} = 1/5$ for momentum approximation and $K_{mom} = 1/10$ and $K_{eng} = 17/70$ for energy approximation [10–21]. Nonlinear fluid forces are obtained by synchronous circular centric-orbit (CCO) motion of the system for a given unbalance. To demonstrate the results of a nonlinear asymmetric system, some of the parameters are taken as: $f = 0.8165$, $f_p = 0.7071$ and $n = 1$. The value of α obtained using Eq. (28) is 0.75 for $\Omega = 0$. Unbalance parameter $U = 0.13$ is considered to get the CCO condition. The response of rotor and damper are presented after normalizing with U . The required optimum damping is calculated using Eq. (29) for an optimum value of $B = 0.177$ for laminar flow without inertial contribution. As earlier, three different damping ratios are considered here to plot the rotor and damper responses. These are, under-damping

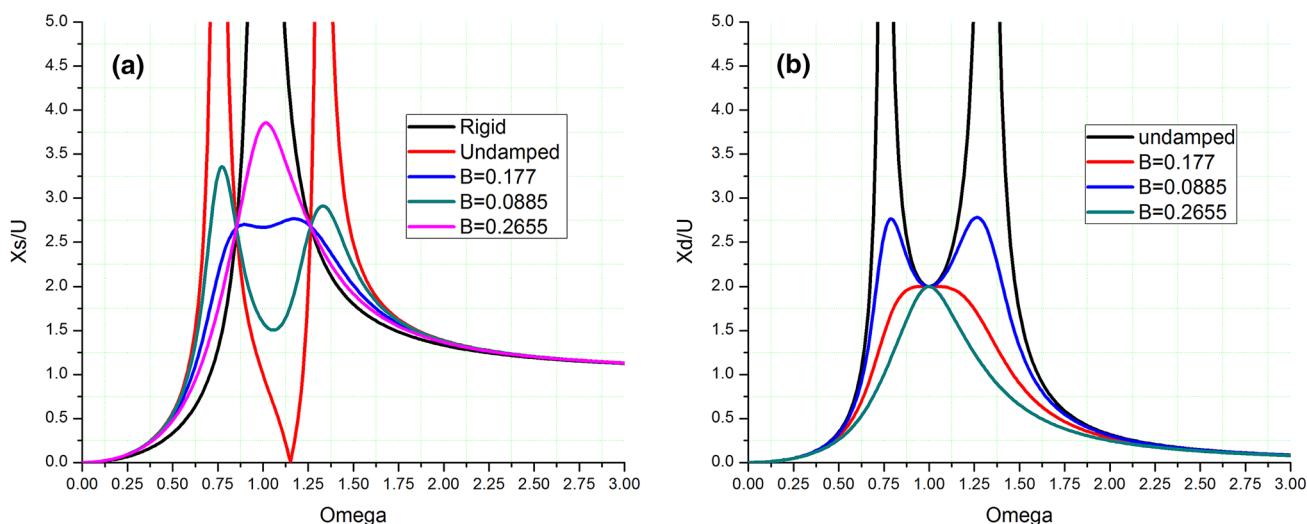


Fig. 9 Results of Case Study-3: **a** responses of nonlinear asymmetric rotor and **b** damper ($f=0.8165, f_p=7071$ and $\alpha=0.75$)

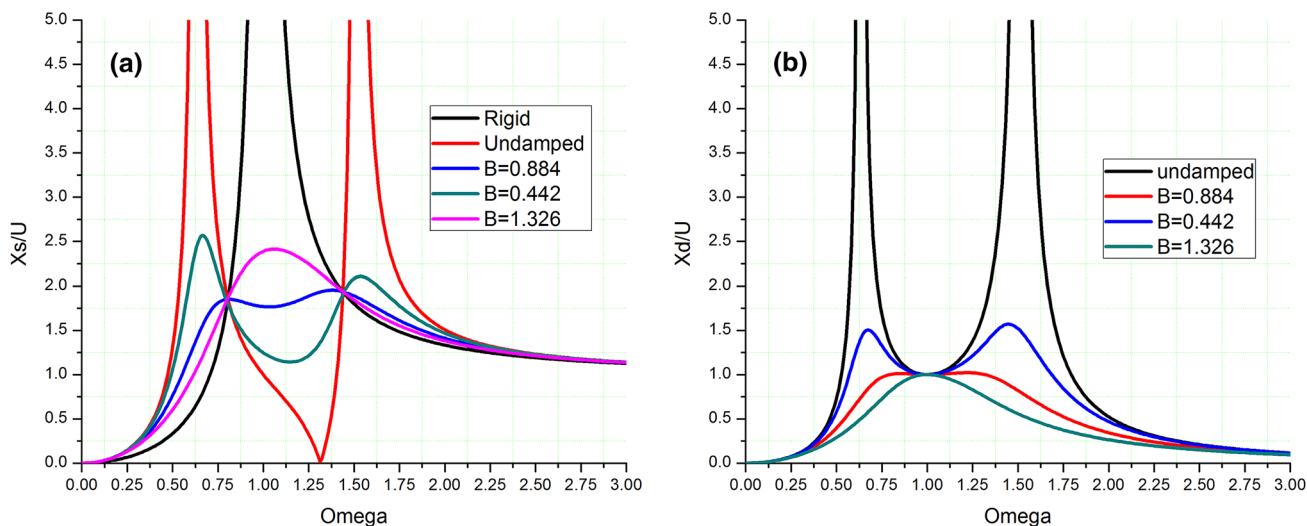


Fig. 10 Results of Case Study-3: **a** responses of nonlinear symmetric rotor and **b** damper ($f=1$ and $\alpha=1$)

case $\xi_1 = 0.5B$, optimum damping, B and over-damping case, $\xi_2 = 1.5B$. Cross-over frequencies are obtained from Eq. (27) as $\Omega P = 0.6278$ and $\Omega Q = 1.275$. Amplitude at cross-over points can be obtained from undamped response of the system by using Eq. (25) and is calculated as 2.70.

Figure 9a shows response of a nonlinear asymmetric rotor for five different conditions. These are (i) response of a rigid rotor, (ii) undamped tuned rotor, (iii) tuned optimum damping ($B=0.177$), (iv) tuned under-damping ($B=0.0885$) and (v) tuned over-damping ($B=0.2655$) conditions. Similarly, Fig. 9b shows response of damper, at four different conditions, which includes tuned undamped damper response,

tuned optimum damper response, tuned under-damping and tuned over-damping conditions. Figure 10a shows the response of a nonlinear symmetric rotor for five different conditions discussed above. These are tuned optimum damping ($B=0.884$), tuned under-damping ($B=0.442$), tuned over-damping conditions ($B=1.326$). Similarly, Fig. 10b shows the response of the damper, at four different conditions as discussed in asymmetric system. Not many changes in rotor and damper responses are observed due to consideration of momentum and energy approximations in nonlinear fluid model. As the present case study deals with a

low Reynolds number, contribution of inertia effect also is negligible in present analysis.

Discussion and Conclusions

Present work shows the development of a close form solution to find out the tuning parameters of an asymmetric flexible rotor with SFD system to cross over the bending critical speeds. Both linear and nonlinear models are considered to find the responses of rotor and damper for both symmetric and asymmetric rotor system. Theoretical modeling of SFD forces is carried out which includes viscous, inertial and temporal contributions under laminar and turbulent conditions. Reynolds equation with short damper approximation is used to derive the SFD coefficients. Calculations of damper forces are done using 2π film approximation with turbulent conditions. Results show that tuning criteria of symmetric rotor is different from asymmetric rotor. Table 2 shows the summary of all the tuning parameters of symmetric, asymmetric linear and nonlinear systems. Some of the conclusions drawn from the present work are as follows.

Symmetric System

For a symmetric system, tuning criteria has to satisfy $f=1$. In case of nonlinear system, physical mass of damper needs to be reduced to take into account the contribution of additional fluid film damper mass. Damper mass increases with the increase in retainer spring stiffness to keep the frequency ratio as one.

Required damping is underestimated if calculated using linear system, in comparison to nonlinear system. However, this difference reduces at higher operating speed.

Cross-over amplitude is one in case of zero stiffness of retainer spring. However, it increases with the increase in retainer spring stiffness.

Optimum damping depends on mass ratio of rotor and damper.

Asymmetric System

Higher the f_p , higher the difference in cross-over frequencies and lower the cross-over amplitudes.

Increase in the value of ' n ' reduces the cross-over amplitudes of the rotor at fixed retainer spring stiffness. However, the cross-over amplitude decreases with the decrease in retainer spring stiffness.

Required optimum damping increases with the increase in the value of ' n ' and decrease the value of retainer spring stiffness.

Optimum damping depends on stiffness of shaft and mass ratio.

References

- Den Hartog JP (1985) Mechanical vibrations, 4th edn. Dover, New York
- Randall SE, Halsted DM, Taylor DL (1981) Optimal vibration absorbers for linear damper systems. *J Mech Design* 103:908–913
- Liu K, Liu J (2005) The damped dynamic vibration absorbers: revisited and new result. *J Sound Vibrat* 284:1181–1189
- Febbo M, Vera SA (2008) Optimization of a two degree of freedom system acting as a dynamic vibration absorber. *J Vibrat Acoust* 130:1–11
- Gunter EJ (1970) Influence of flexibly mounted rolling element bearings on rotor response, part I linear analysis. *J Lubricat Technol* 92:59–69
- Kirk RG, Gunter EJ (1972) The effect of support flexibility and damping on the synchronous response of single mass flexible rotor. *J Eng Ind* 94(1):221–232
- Cunningham RE, Cunningham DP, Gunter EJ (1975) Design of a squeeze-film dampers for a multi-mass flexible rotor. *J Eng Ind* 97(4):1383–1389
- Pilkey WD, Wang BP, Vannoy D (1976) Efficient optimal design of suspension systems for rotating shafts. *J Eng Ind* 98(3):1026–1029
- Jawaid II-H (2005) Bifurcations of a flexible rotor response in squeeze-film dampers without centering springs. *Chaos Sol Fract* 24:583–596
- Jawaid II-H (2009) Bifurcations in the response of a flexible rotor in squeeze-film dampers with retainer springs. *Chaos Sol Fract* 39:519–532
- Rao JS (2018) Rotor dynamics, 3rd edn. New age International publications, Bengaluru
- Rabinowitz MD, and Hahn EJ (1977) Steady state performance of squeeze film damper supported flexible rotors. *J Eng Power* 552–558
- Rabinowitz MD, Hahn EJ (1983) Optimal design of squeeze film supports for flexible rotors. *J Eng Power* 105:487–494
- Rabinowitz MD, Hahn EJ (1983) Experimental evaluation of squeeze film supported flexible rotors. *J Eng Power* 105:495–503
- McLean LJ, Hahn EJ (1983) Unbalance behavior of squeeze film damped multi-mass flexible rotor bearing systems. *J Lubricat Technol* 105:22–27
- McLean LJ, Hahn EJ (1985) Stability of squeeze film damped multi-mass flexible rotor bearing systems. *J Tribol* 107:402–409
- Chen WJ, Rajan M, Rajan SD, Nelson HD (1988) The optimal design of squeeze film dampers for flexible rotor systems. *J Mech Trans Automat Design* 110:166–174
- Zhu CS, Robb DA, Ewins DJ (2002) Analysis of the multiple-resolution response of a flexible rotor supported on non-linear squeeze film dampers. *J Sound Vibrat* 252(3):389–408
- EI-Shafei A, Yakoub RYK (2002) Optimum design of squeeze film dampers supporting multiple mode rotors. *J Eng Gas Turb Power* 124:992–1001
- Pietra LD, Adiletta G (2002) The squeeze film damper over four decades of investigations. Part I: characteristics and operating features. *Shock Vibr Dig* 34:3–26
- Adiletta G, Pietra LD (2002) The squeeze film damper over four decades of investigations. Part II: rotor dynamic analyses with rigid and flexible rotors. *Shock Vibr Dig* 34:97–126
- Qingchang T, Chang Y, Wang L (1997) Effect of a circumferential feeding groove on fluid force in short squeeze film dampers. *Tribol Int* 30:409–416
- Qingchang T, Xiaohua L (1999) Analytical study on effect of a circumferential feeding groove on unbalance response of a flexible rotor in squeeze film damper. *Tribol Int* 32:559–566

24. Rezvani MA, Hahn EJ (1996) An experimental evaluation of squeeze film dampers without centralizing springs. *Tribol Int* 29(1):51–59
25. Rezvani MA, Hahn EJ (2000) Floating ring squeeze film damper: theoretical analysis. *Tribol Int* 33:249–258
26. Hai-Lun Z, Gui-Huo L, Guo C, Fei W (2013) Analysis of the nonlinear dynamic response of a rotor supported on ball bearings with floating-ring squeeze film dampers. *Mech Mach Theory* 59:65–77
27. Giovanni A (2015) Bifurcating behaviour of a rotor on two-lobe wave squeeze film damper. *Tribol Int* 92:72–83
28. Wang J, Feng N, Meng G, Hahn EJ (2006) Vibration control of rotor by squeeze film damper with magnetorheological fluid. *J Intell Mater Syst Struct* 17:353–357
29. Jaroslav Z, Petr F, Paola F (2017) A new mathematical model of a short magnetorheological squeeze film damper for rotordynamic applications based on a bilinear oil representation—derivation of the governing equations. *Appl Math Model* 52:558–575
30. Siva Srinivas R, Tiwari R, Kannababu Ch (2018) Application of active magnetic bearings in flexible rotordynamic systems—a state-of-the-art review. *Mech Syst Signal Process* 106:537–572
31. Heidari HR, Safarpour P (2016) Design and modeling of a novel active squeeze film damper. *Mech Mach Theory* 105:235–243
32. Zhifei H, Qian D, Wei Z (2019) Dynamical analysis of an elastic ring squeeze film damper-rotor system. *Mech Mach Theory* 131:406–419
33. Wei Z, Bingbing H, Xiang L, Jianqiao S, Qian D (2019) Multiple-objective design optimization of squirrel cage for squeeze film damper by using cell mapping method and experimental validation. *Mech Mach Theory* 132:66–79
34. Muszynska A (1986) Whirl and whip rotor/bearing stability problems. *J Sound Vibrat* 110(3):443–462
35. Zhang J, Ellis J, Roberts JB (1993) Observations on the nonlinear fluid forces in short cylindrical squeeze film dampers. *ASME J Tribol* 115:692–698
36. Shaik K, Dutta BK, Gouthaman G (2019) Experimental and analytical investigation of short squeeze-film damper (SFD) under circular-centered orbit (CCO) motion. *J Vibrat Eng Technol*. <https://doi.org/10.1007/s42417-019-00100-9>
37. Ku C-P, Tichy JA (1987) Application of the $k-\epsilon$ turbulence model to the squeeze film damper. *ASME J Tribol* 109:164–168
38. Booker JF (1965) A table of the journal bearing integral. *ASME J Basic Eng* 1965:533–535

Publisher's Note Springer Nature remains neutral with regard to jurisdictional claims in published maps and institutional affiliations.